EUROPEAN FUSION DEVELOPMENT AGREEMENT

JET

EFDA–JET–CP(07)03/29

C.D. Challis, E. Joffrin, T. Luce, P. Buratti, P de Vries, J. Hobirk, B. Alper, M. Brix, R. Felton, J. Ferron, C. Giroud, M. Gryaznevich, N. Hawkes, T.C. Hender, D. Howell, J. Menard, M. Murakami, E. Rachlew, S. Saarelma, S. Sharapov, O. Tudisco, I. Voitsekhovitch, O. Zimmermann and JET EFDA contributors

High β_N JET H-modes for Steady-State Application

High β_N JET H-modes for Steady-State Application

C.D. Challis[1], E. Joffrin[2], T. Luce[3], P. Buratti[4], P de Vries[1], J. Hobirk[5], B. Alper[1], M. Brix[1], R. Felton[1], J. Ferron[3], C. Giroud[1], M. Gryaznevich[1], N. Hawkes[1], T.C. Hender[1], D. Howell[1], J. Menard[6], M. Murakami[7], E. Rachlew[8], S. Saarelma[1], S. Sharapov[1], O. Tudisco[4], I. Voitsekhovitch[1], O. Zimmermann[9] and JET EFDA contributors*

[1]EURATOM/UKAEA Fusion Association, Culham Science Centre, Abingdon, OX14 3DB, UK
[2]Association Euration-CEA, DSM/DRFC, Cadarache F-13108, France
[3]General Atomics, PO Box 85608, San Diego, Ca 92186-5608, USA
[4]EURATOM-ENEA Association, C.R. Frascati, CP65, 00044 Frascati, Italy
[5]Max-Planck-Institut für Plasmaphysik, Euratom Association, 85748 Garching, Germany
[6]Princeton Plasma Physics Laboratory, New Jersey 08543-0451, USA
[7]Oak Ridge National Laboratory, Oak Ridge, Tennessee 37831-6169, USA
[8]Association EURATOM-VR, Royal Institute of Technology, 10691 Stockholm, Sweden
[9]Forschungzentrum Jülich, Institut für Plasmaphysik, Association Euratom-FZJ, Germany
** See annex of M.L. Watkins et al, "Overview of JET Results ",*
(Proc. 21st IAEA Fusion Energy Conference, Chengdu, China (2006)).

Preprint of Paper to be submitted for publication in Proceedings of the
34th EPS Conference on Plasma Physics,
(Warsaw, Poland 2nd - 6th July 2007)

1. INTRODUCTION

An efficient steady-state tokamak fusion power plant requires stable operation at high plasma pressure without excessive recirculating power. Access to high β_N with a q profile compatible with large bootstrap current is, therefore, highly desirable. Recent experiments at JET have investigated the access to high β_N for plasmas with H-mode edge and $q_0 \geq 1$. The 1.2MA/1.8T ($q_{95} \approx 5$) plasmas were formed by the initial inductive ramp-up phase, similar to experiments developed at DIII-D [1]. LHCD or ICRH was added in some discharges and the initial current ramp rate varied to tailor the q profile shape as the current penetrated towards the plasma centre. The resulting target q profile at the start of the main NBI heating phase had low or reversed magnetic shear in the core and the minimum value of q (q_{min}) was adjusted using the start time of the NBI pulse. The time evolution of a typical pulse is shown in figure 1. The initial rise in β was provided by pre-programmed NBI power. Real-time control was triggered at $\beta_N = 1$ and b_N was then controlled by feedback on the NBI power. In these experiments $\beta_N \approx 3$ was sustained for up to ~$18\tau_E$ and $\beta_N \approx 2.8$ for up to ~$35\tau_E$, which is of the order of the resistive time and was limited by the allowed NBI pulse length for this particular configuration.

2. STABILITY

Many discharges were obtained with total b_N above the no-wall b-limit, determined theoretically by modelling and empirically by observing resonant field amplification of an externally applied magnetic perturbation [3]. This latter technique showed that, for the case in figure 1, β_N remained above the no-wall limit during t = 4.45-11.45s. In practice the achievable b was limited in these experiments by an n = 1 MHD instability that resulted in significant loss of confinement. The sensitivity of this limit to the q profile shape was systematically investigated by varying the start time of the NBI pulse and the results are shown in figure 2. These cases have a slow current ramp, as illustrated by the example in figure 1, and are without either ICRH or LHCD preheating.

The effect of varying the NBI start time is to partially “freeze” the current density profile before it has fully diffused. q_{min} at the start of the NBI heating has been estimated from the start of sawtooth activity in Ohmic reference pulses (indicating q = 1 at t ≈ 4.3s) and from the time of grand Alfvén cascades [4] (indicating $q_{min} = 2$ at t ≈ 2.6s). The slow evolution of the q profile during the main heating phase means that the value of q_{min} at the onset of the n = 1 mode will be slightly different from the value indicated in figure 2. Nevertheless, the correlation between q_{min} and achievable b_N is clearly seen with higher β_N obtained at low q_{min}. This observation is consistent with modelling predictions for β limitations in these conditions [3] although the exact nature of the n = 1 instability has not yet been unambiguously identified.

3. CONFINEMENT

A triangular plasma configuration (δ = 0.34−0.4) was used with good H-mode confinement (up to $H_{IPB98(y,2)} \approx 1.1$ and $H_{ITER89L-P} \approx 2.1$) at ITER (steady-state) relevant q_{95} (≈5) leading to a steady fusion figure of merit $G \approx 0.25$ ($\int H_{ITER89L-P} \times \beta_N/q_{95}^2$). The plasma edge was characterised by type-I ELMs and the density was 50–70% of the Greenwald value. In this regime very steep temperature gradients associated with 'strong' ITBs were not seen.

The dependence of the plasma energy confinement on the q profile shape has been studied in this plasma regime. Figure 3 shows the confinement H factor with respect to the ITER89L-P L-mode scaling averaged over the period 2-3s after the start of the NBI heating. This is shown as a function of NBI start time for pulses with NBI power in the range 7.5-12.5MW during the same averaging period and, again, no LHCD or ICRH. Cases with gas fuelling or significant n = 1 MHD during the averaging period were also deselected from the dataset shown in figure 3 as both of these effects were seen to degrade the confinement. Figure 3 shows a systematic increase in confinement with NBI start time. Plasmas with different initial current ramp rates were included, but the NBI start time was found to be the dominant factor in varying q_{min}.

The influence of the q profile on the pressure profile can be seen most dramatically in the time evolution of the pulses with the earliest heating, because they exhibit the largest variation in q profile shape. Figure 4 shows the evolution of the electron pressure profile for a pulse with a steady 10MW of NBI heating starting at t_{nbi} = 2s. After 0.5s the pressure profile is still flat, despite the fact that this time exceeds both the NBI fast ion slowing down and plasma energy confinement times. It takes several seconds for the pressure profile to become fully peaked, which is more consistent with the timescale for current to penetrate to the plasma core. Equivalent profiles for a plasma with t_{nbi} = 3s are shown in figure 4 showing the improved core pressure with later heating. Thus is can be seen that the global confinement and core pressure both increase as q is reduced in the plasma core.

4. CURRENT DRIVE

It is estimated using TRANSP that about a third of the plasma current was provided by the bootstrap mechanism in plasmas at $\beta_N \approx 3$ and, with the on-axis NBI current, about 50-70% of the total current was driven non-inductively. Plasmas with late NBI timing (t ≈ 4s with q_0 close to unity – see figure 2) sometimes exhibited fishbone instabilities near the start of the NBI phase. The disappearance of these modes and the continued absence of sawteeth for a resistive time is consistent with q_0 remaining close to or above 1 due to the off-axis bootstrap current.

CONCLUSIONS

These experiments address the q profile optimisation for stability in ITER (steady-state) relevant condition, despite the fact that the H-factor is, so far, below the required value. The optimum stability and confinement in this regime (i.e. without a 'strong' ITB) was achieved with low q (but ≥1) in the plasma core at the start of the NBI heating. This good performance was maintained for about a resistive time without the need for externally driven off-axis current to avoid sawteeth. A larger bootstrap fraction would be expected if the same value of total β_N were achieved with a lower fraction of the plasma stored energy being due to fast particles. This would be expected to increase q_{min}, which appears unfavourable for confinement and stability. Under these circumstances it might be desirable to provide externally driven non-inductive current in the central region of the plasma to optimise performance. It should be noted that the current drive system optimisation may be entirely different for plasmas relying on ITBs to provide improved confinement, for which low or negative magnetic shear at large plasma radius may be required [5].

ACKNOWLEDGEMENTS

This work was funded partly by the United Kingdom Engineering and Physical Sciences Research Council and by the European Communities under the contract of Association between EURATOM and UKAEA. The views and opinions expressed herein do not necessarily reflect those of the European Commission. This work was carried out within the framework of the European Fusion Development Agreement.

REFERENCES

[1]. T.C. Luce et al Nucl. Fusion **45** (2005) S86

[2]. R.J. Goldstona et al J. Comput. Phys. **43** (1981) 61

[3]. M. Gryaznevich et al this Conference (P5-145)

[4]. S.E Sharapov et al Phys. Lett. A **289** (2001) 127

[5]. J. Mailloux et al this Conference (P4-151)

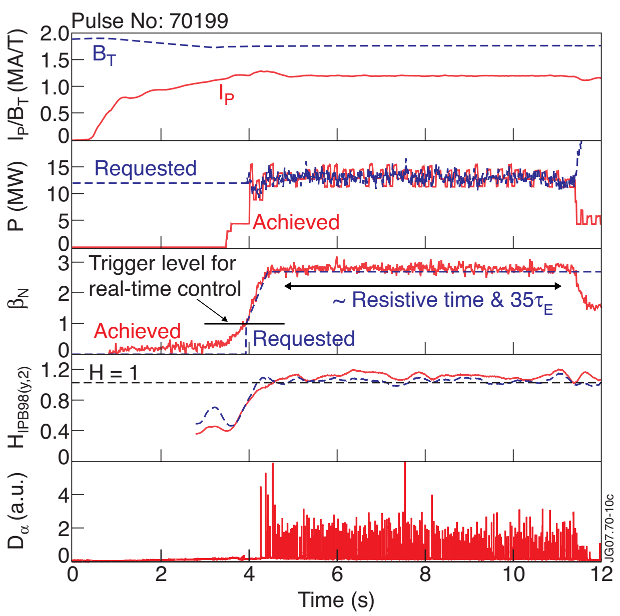

Figure 1: Time evolution of a typical high β_N pulse showing plasma current and magnetic field; requested and achieved NBI power; requested and achieved b_N; $H_{IPB98(y,2)}$; and D_α, showing type I ELMs. $H_{ITER98(y,2)}$ was evaluated using thermal stored energy from pressure profile integration (red) and $W_{diamagnetic}$-1.5×$W_{\perp fast}$ using TRANSP NBI model [2] (blue).

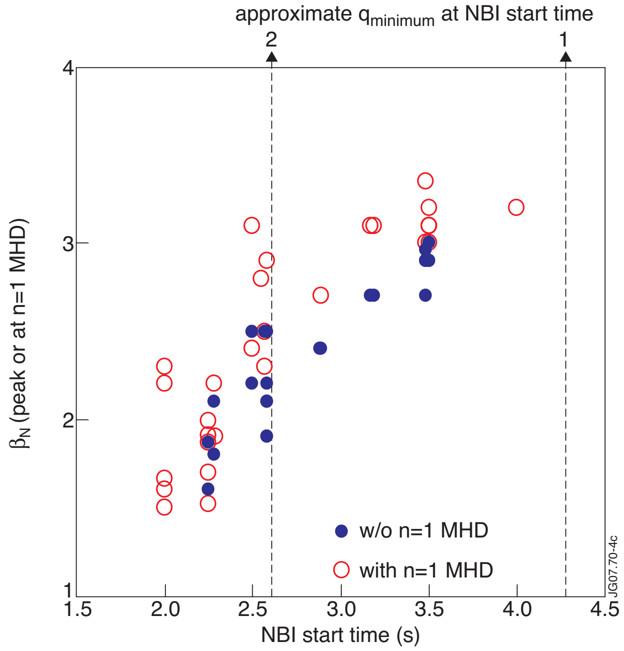

Figure 2. Maximum β_N (or the value at the start of performance limiting n=1 MHD activity) plotted against the start time of the main NBI heating.

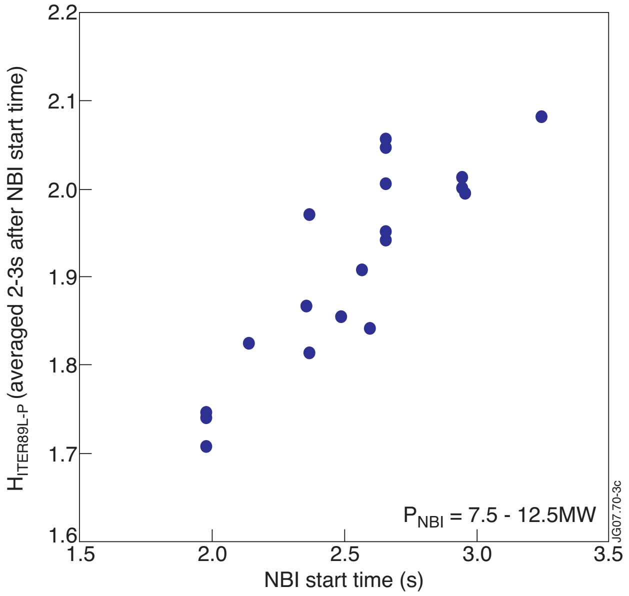

Figure 3. $H_{ITER89L-P}$ averaged over the period 2-3s after the start of NBI plotted against NBI start time.

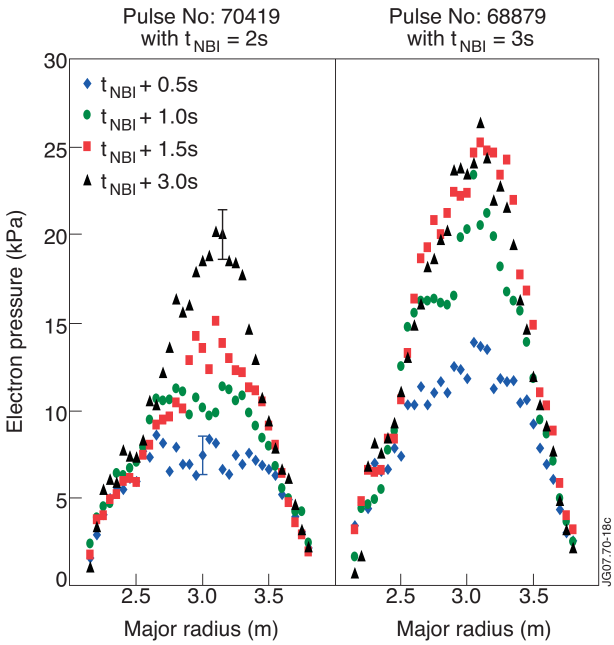

Figure 4. Electron pressure profiles measured using LIDAR showing the different evolution for pulses with different NBI start times. Each profile averaged over two points ±125ms.